Probability Distribution of a Signal's Peak Time in a Molecular Diffusive Media

Ethungshan Shitiri, *Member, IEEE*, H. Birkan Yilmaz, *Member, IEEE*, and Ho-Shin Cho, *Senior Member, IEEE*

***Abstract*— The peak time of a received signal in a molecular channel is random and generally assumed to follow the Normal distribution. However, the untested validity of the assumption motivates this letter. Considering an absorbing receiver placed in a free-diffusion molecular communication via diffusion (MCvD) system, we analyze the randomness in terms of the distribution of the peak time using simulated data and define one of the parameters. In addition, we derive the semi-analytical expressions of the distribution by using Poisson and Normal approximations of the absorbed molecules. Through numerical analysis, we evaluate the accuracy of the models and demonstrate that the Poisson model achieves a better fit. The key finding is that the distribution has extreme values resulting in a heavy right-tail and this information can be a useful tool to develop improved channel models.**

***Index Terms*— Diffusion, distribution model, molecular communication, peak time.**

I. Introduction

MOLECULAR **c**ommunication (MC) is a communication paradigm wherein the information is encoded on molecules — a feature that distinguishes it from conventional communication paradigms, such as electromagnetic-wave based communication [1]. MC, therefore, has opened up the possibility of realizing communication networks in harsh environments (e.g., living tissues), where the conventional methods may fail and biocompatibility is critical. Another unique feature of MC is the fluidic media, where the molecules propagate via diffusion and thus the name **m**olecular **c**ommunication **v**ia **d**iffusion (MCvD) [2]. Thus, molecules traverse through thermal vibrations and collisions with other smaller molecules present in the environment, which is commonly described by Brownian motion [3]. Diffusion may occur with and without flow in the media, namely *assisted-diffusion* and *free-diffusion* [1], respectively. This letter focus on the latter.

Among the envisioned encoding techniques (concentration, type, number, and time), concentration encoding is widely studied because of its simplicity [4]. In its most basic form, namely *binary concentration-shift keying*, symbol '1' is encoded by the release of molecules and no such release for symbol '0'. To decode a symbol, a receiver samples the received signal at some time instant at which a peak in the concentration (maximum number of molecules) is anticipated [5]. If the sampled value is above a desired threshold, the symbol '1' is decoded, else symbol '0' is decoded. The aforementioned time instant at which the peak occurs is referred to as the *peak time*, which is also considered to be the time taken by a signal emitted at the transmitter to reach the receiver [2]. Besides decoding purposes, knowledge of the peak time is useful to estimate channel parameters [6]–[10] and also to perform networking functions [11].

The measured peak is reported to be noisy because of the stochastic nature of the channel [12, p. 57]. Subsequently, the observed peak time will vary for every symbol slot at the receiver side that correspond to multiple emissions at the transmitter, and hence the peak time is random. In [5], considering a passive receiver, the authors indicate that the distribution is a Poisson distribution, but detailed analysis about the parameters are not provided. Moreover, for computational purposes, studies commonly assume it to be a Normal distribution [8], [13]. An accurate description about the distribution of the peak time can be an effective tool to optimize system designs. An area that can immediately benefit from the knowledge of the distribution is symbol detection. Multiple sampling does not necessarily ensure accurate measurements of the peak time, but multiple sampling performed in the vicinity of the expected peak time does. This can lead to a reduction in the number of sampling intervals that is favorable to the power-limited receiver. In particular, estimating the amount of variance in the peak time can be a useful tool to optimize the number of sampling intervals with a potential of lowering the complexity of the receiver.

Motivated by the aforementioned reasons, in this study, we investigate the distribution of the peak time considering an absorbing receiver in a free-diffusion MCvD system. Briefly, we derive the semi-analytic expressions of the distribution when a signal is emitted at the transmitter using both Poisson and Normal approximations of the number of absorbed molecules. Then, we use simulated data from L Monte-Carlo replications that are analogous to the emission of L bit '1' signals at the transmitter to analyze the histogram of the distribution and its parameters for various physical settings.

II. System Model

We consider a point-to-spherical MCvD system as illustrated in Fig. 1. It consists of a spherical receiver (Rx) that is located at a distance d from a point transmitter (Tx) in

Manuscript received August 21, 2021; revised September 18, 2021 and September 23, 2021; accepted September 23, 2021. Date of publication September 27, 2021; date of current version December 10, 2021. This study was supported by the National Research Foundation of Korea (NRF) grant funded by the Korean Government (MSIT) (2017R1A2B4002622 and 2021R1A2C1003507). The associate editor coordinating the review of this letter and approving it for publication was A. Noel. *(Corresponding author: Ho-Shin Cho.)*

Ethungshan Shitiri and Ho-Shin Cho are with the School of Electronic and Electrical Engineering, Kyungpook National University, Daegu 41566, South Korea (e-mail: ethungshan@ee.knu.ac.kr; hscho@ee.knu.ac.kr).

H. Birkan Yilmaz is with the Department of Computer Engineering, Boğaziçi University, 34342 Istanbul, Turkey (e-mail: birkan.yilmaz@boun.edu.tr).

Digital Object Identifier 10.1109/LCOMM.2021.3115724

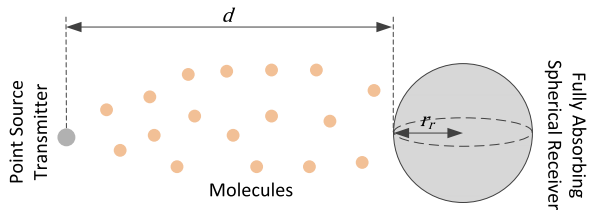

Fig. 1. MCvD system model. Note: Not drawn to scale.

an unbounded 3-D environment. The transmitter emits N^{Tx} number of molecules, emulating an impulse signal, into the environment, which is analogous to the instantaneous release of molecules from a vesicle [14]. The emitted molecules diffuse independently, governed by the dynamics of the Brownian motion; and by borrowing the mathematical expressions from [2], we can observe the location of a molecule at time t as

$$r[t] = r[t-\Delta t] + (\Delta r_1, \Delta r_2, \Delta r_3),\ \Delta r_i \sim \mathcal{N}(0,\ 2D\Delta t), \quad (1)$$

where $r[t]$, r_i, D, and Δt are the location vector at time t, i-th component of the location vector, diffusion coefficient, and the time step, respectively. $\mathcal{N}(0, \sigma^2)$ is the Normal distribution with mean 0 and variance $2D\Delta t$. The receiver is considered to be a perfectly absorbing body and is able to keep track of the absorbed molecules' count in each sampling interval. Moreover, the receiver uses a simple peak detector that can determine the maximum among the sampled counts. From [2], the hitting rate of the molecules at the receiver, $f_{\text{hit}}(t|r_r, d, D)$, and the fraction of molecules absorbed by the receiver, $F_{\text{hit}}(d, t)$, until time t can be expressed as

$$f_{\text{hit}}(t|r_r, d, D) = \left(\frac{r_r}{d + r_r}\right) \frac{d}{\sqrt{4\pi D t^3}} \exp^{-d^2/4Dt} \quad (2)$$

$$\text{and } F_{\text{hit}}(d, t) = \left(\frac{r_r}{d + r_r}\right) 2\Phi\left(\frac{-d}{\sqrt{2Dt}}\right), \quad (3)$$

respectively, where r_r is the radius of the receiver and $\Phi(\cdot)$ denotes the cumulative distribution function of the standard Normal distribution. Let T_{peak} denote the peak time. Then, the expected peak time, which we denote as $\mathbb{E}[T_{\text{peak}}]$, is proportional to the distance squared and inversely proportional to the diffusion coefficient and can be written as [2]

$$\mathbb{E}[T_{\text{peak}}] = \frac{d^2}{6D}, \quad (4)$$

where $\mathbb{E}[\cdot]$ is the expectation operator. In what follows, we derive the semi-analytical expressions of the probability distribution of T_{peak} when a signal is emitted at the Tx.

III. Peak Time Distribution

A. Theoretical Approach: Single Emission Case

Let us consider that at time $t = 0$, Tx releases N^{Tx} number of molecules, which arrive at the Rx following (1). Time is discretized into K equal time intervals, such that the k-th time interval can be represented by $t_k = (t_k^-, t_k^+)$ with a duration equal to $\Delta t_s = t_k^+ - t_k^-$. Then, we can write the expected number of absorbed molecules $N^{\text{Rx}}[k]$ at the k-th time interval as

$$\mathbb{E}\big[N^{\text{Rx}}[k]\big] = N^{\text{Tx}} \cdot \Big(F_{\text{hit}}(d, t_k^+) - F_{\text{hit}}(d, t_k^-)\Big). \quad (5)$$

As the molecules move independently, the distribution of the number of absorbed molecules in the K intervals can be modeled as a Multinomial distribution $\mathbf{X} \sim \mathcal{M}(N^{\text{Tx}}, \mathbf{p})$ [15, p. 197]. Here, $\mathbf{X} := \big[N^{\text{Rx}}[1], \cdots, N^{\text{Rx}}[K]\big]$, and $\mathcal{M}(n, \mathbf{p})$ denotes the Multinomial distribution with n independent trials and probabilities $\mathbf{p} := [p_1, \cdots, p_K]$, where the p_k values are normalized version of $\big(F_{\text{hit}}(d, t_k^+) - F_{\text{hit}}(d, t_k^-)\big)$. Furthermore, for tractability, we assume independence between consecutive intervals [16]. Then, when $K \longrightarrow \infty$, we can approximate the Multinomial random vector by individual Binomial distribution. Hence, $N^{\text{Rx}}[k] \sim \mathcal{B}\Big(N^{\text{Tx}}, F_{\text{hit}}(d, t_k^+) - F_{\text{hit}}(d, t_k^-)\Big)$, where $\mathcal{B}(n, p)$ is the Binomial distribution with n independent trials and probability p. Furthermore, if $N^{\text{Tx}} \longrightarrow \infty$ and $\big(F_{\text{hit}}(d, t_k^+) - F_{\text{hit}}(d, t_k^-)\big) \longrightarrow 0$, then the Binomial distribution can be approximated by the Poisson distribution [17]. Thus, the random variable of $N^{\text{Rx}}[k]$ molecules can be expressed as

$$N^{\text{Rx}}[k] \sim \mathscr{P}(\lambda_k), \quad (6)$$

where $\mathscr{P}(\lambda)$ denotes the Poisson distribution with mean λ and $\lambda_k = \mathbb{E}\big[N^{\text{Rx}}[k]\big]$. Similarly, applying the Normal approximation of the Binomial, we obtain

$$N^{\text{Rx}}[k] \sim \mathcal{N}(\mu_k, \sigma_k^2), \quad (7)$$

where $\mathcal{N}(\mu, \sigma^2)$ is the Normal distribution with mean μ and variance σ^2; and $\mu_k = \mathbb{E}\big[N^{\text{Rx}}[k]\big]$ and $\sigma_k^2 = \mathbb{E}\big[N^{\text{Rx}}[k]\big]\big(1 - F_{\text{hit}}(d, t_k^+) + F_{\text{hit}}(d, t_k^-)\big)$. The peak time derived from the observed samples can then be defined as

$$T_{\text{peak}} = \left(\underset{k=1,2,\cdots,K}{\text{argmax}}\ N^{\text{Rx}}[k] - 0.5\right)\Delta t_s, \quad (8)$$

where the $\text{argmax}(\cdot)$ operator extracts the index of the interval that holds the maximum N^{Rx} and the negative constant 0.5 gives the midpoint of that interval. Note that owing to the stochasticity in diffusion process, the interval with the maximum N^{Rx} changes for each release of Q molecules at the transmitter; hence T_{peak} is random. In what follows, we derive the probability of each k-th time interval holding the maximum number of molecules. For conciseness, we shall use Q_k to denote the event "`interval k holds the maximum` N^{Rx} `among K time intervals`". Then, the probability distribution of Q_k under (6) can be written as

$$\begin{aligned}\Pr(Q_k)^{\text{poisson}} &= \sum_{i=1}^{N^{\text{Rx}}(t_K^+)} \Pr\big(N^{\text{Rx}}[k] = i\big) \prod_{j \neq k}^{K} \Pr\big(N^{\text{Rx}}[j] < i\big), \\ &= \sum_{i=1}^{N^{\text{Rx}}(t_K^+)} f_{\mathscr{P}}(i, \lambda_k) \prod_{j \neq k}^{K} F_{\mathscr{P}}(i-1, \lambda_j), \end{aligned} \quad (9)$$

where $N^{\text{Rx}}(t_K^+) = \sum_{k=1}^{K} N^{\text{Rx}}[k]$ is the total number of the molecules absorbed until time t_K^+ and $f_{\mathscr{P}}(x, \lambda)$ and $F_{\mathscr{P}}(x, \lambda)$ are the probability mass function and the cumulative distribution function of the Poisson distribution, respectively.

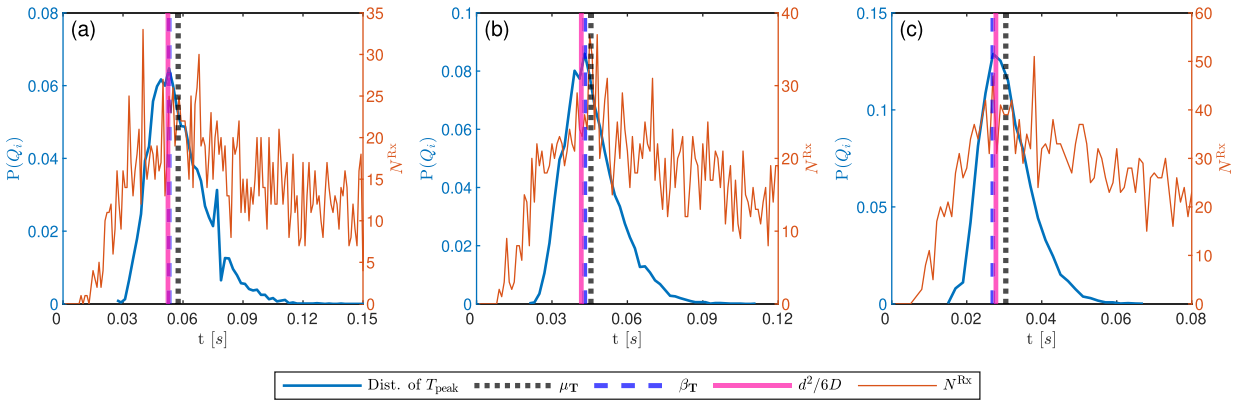

Fig. 2. Distribution of T_{peak} with $d = 5$ μm for (a) $D = 79.4$ $\mu\mathrm{m}^2/\mathrm{s}$ (b) $D =$ $\mu\mathrm{m}^2/\mathrm{s}$ (c) $D = 150$ $\mu\mathrm{m}^2/\mathrm{s}$. $\mu_{\mathbf{T}}$ and $\beta_{\mathbf{T}}$ (denoted by vertical lines) are the mean and mode, respectively. i denotes the i-th time interval as defined in (13). $r_r = 10$ μm, $N^{\mathrm{Tx}} = 10000$ molecules, $\Delta t = 0.1$ ms, $\Delta t_s = 1$ ms, and $L = 10000$ replications. Each replication last 1 s. Unless specified otherwise, these parameter values are used throughout the letter. Data in this figure are from a single $L = 10000$ replications, the remaining figures' data points are averages of ten $L = 10000$ replications.

Similarly, the probability distribution of Q_k under (7) can be written as

$$\Pr(Q_k)^{\mathrm{normal}} = \sum_{i=1}^{N^{\mathrm{Rx}}(t_K^+)} f_{\mathcal{N}}(i, \mu_k, \sigma_k^2) \prod_{j \neq k}^{K} F_{\mathcal{N}}(i - 0.5, \mu_j, \sigma_j^2), \tag{10}$$

where $f_{\mathcal{N}}(x, \mu, \sigma^2)$ and $F_{\mathcal{N}}(x, \mu, \sigma^2)$ are the probability density function and the cumulative distribution function of the Normal distribution, respectively. Please note that the approximations are used for $N^{\mathrm{Rx}}[k]$ and not Q_k. We note that there is no simple closed form solution but (9) and (10) can be evaluated numerically. Given Δt_s and $\Pr(Q_k)$, we can easily compute the distribution of T_{peak} by using (8).

B. Experimental Approach: Multiple Emission Case

Let us consider L replications, which represents the emission of L identical signals at the Tx. We state that the signals are identical to each other since Tx emits the same number of molecules in every emission. Then we denote the estimated T_{peak} of the l-th emission as $\hat{T}_{\mathrm{peak},l}$, which can be expressed as

$$\hat{T}_{\mathrm{peak},l} = (k_l - 0.5)\Delta t_s, \tag{11}$$

where k_l is the index of the interval corresponding to the maximum N^{Rx} in the l-th emission. Now, we can define a new random vector $\mathbf{T}$ as

$$\mathbf{T} := [\hat{T}_{\mathrm{peak},1}, \cdots, \hat{T}_{\mathrm{peak},L}]. \tag{12}$$

Given $\mathbf{T}$, the empirical distribution of T_{peak} can written as

$$\Pr(Q_i)^{\mathrm{sim}} = \frac{N_{T_{\mathrm{peak}}}[i]}{L}, \quad \forall i \in K, \tag{13}$$

where $N_{T_{\mathrm{peak}}}[i]$ is the number of $\hat{T}_{\mathrm{peak}}$ values that fall within the limits of the i-th interval, $\left[t_i^-, t_i^- + \Delta t_s\right)$. Statistically speaking, the empirical $\Pr(Q_i)$ values would exhibit dispersion either from the *average value* and/or the *most recurring value*. The former is called the *mean*, which we denote by $\mu_{\mathbf{T}} = (\int i \Pr(Q_i)^{\mathrm{sim}} di - 0.5) \cdot \Delta t_s$ and the latter is called the *mode*, which we denote by $\beta_{\mathbf{T}} = (\mathrm{argmax}_i \Pr(Q_i)^{\mathrm{sim}} - 0.5) \cdot \Delta t_s$. The amount of dispersion is quantified most commonly by the *standard deviation*, $\sigma_{\mathbf{T}} = \sqrt{(\int i^2 \Pr(Q_i)^{\mathrm{sim}} di - 1) \cdot \Delta t_s - \mu_{\mathbf{T}}^2}$. However, since the distribution is skewed, we calculate the standard deviation using the *method of five-number summary* (the sample median, the first and third quartiles, and the minimum and maximum values) [18]. In what follows, we analyze the probability distribution of the peak time. Note that the data in this study are generated using a particle-based simulator that incorporates the effective geometry Monte Carlo algorithm [19].

IV. Analysis of Peak Time Distribution

Fig. 2 presents the distribution of T_{peak} obtained via simulations. Firstly, we observe that the actual T_{peak} can vary considerably around the expected T_{peak} such that extreme values of T_{peak} can be observed further into the falling slope of N^{Rx}. Secondly, we observe that the distribution is asymmetric that is left-skewed with a heavy right-tail, confirming the existence of extreme values. Moreover, the $\mu_{\mathbf{T}}$ and $\beta_{\mathbf{T}}$ are unequal. These properties fail to meet the criteria of a Normal distribution. Thirdly, we observe that $\beta_{\mathbf{T}}$ is much closer to the expected peak time. Therefore, we posit that

$$\beta_{\mathbf{T}} = \frac{d^2}{6D}. \tag{14}$$

Eq. (14) is verified via simulations as shown in Fig. 3. At this point, we note that the skewed distribution observed here should not be confused with that for timing channels [20]. It differs in terms of what is described, which is the *distribution of the arrival time of a single molecule.* Fig. 4 presents the dispersion in terms of the standard deviation, where, as expected, the deviations from the expected peak time grow with distance.

To verify the estimation precision of the peak time via (11), we determine the 90% confidence intervals. Let $T_{\mathrm{peak}} \in [\delta^*_{\alpha_1}, \delta^*_{\alpha_2}]$ with 90% probability. As generally used, "$*$" represents the bootstraped values. $\delta^*_{\alpha_1}$ and $\delta^*_{\alpha_2}$ denote the bias corrected and accelerated (BC_a) bootstrap confidence intervals that are the $(\alpha_1 K)$th and the $(\alpha_2 K)$th ordered values of the bootstrap replications $\hat{T}^*_{\mathrm{peak}}$ distribution, respectively. Descriptions of α_1 and α_2 are given in [21, eq. (14.10)].

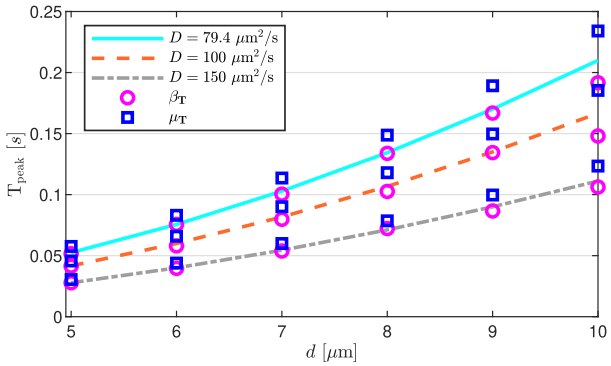

Fig. 3. Expected T_{peak} from (4) (lines). Squares and circles represent $\mu_{\mathbf{T}}$ and $\beta_{\mathbf{T}}$ from simulations, respectively.

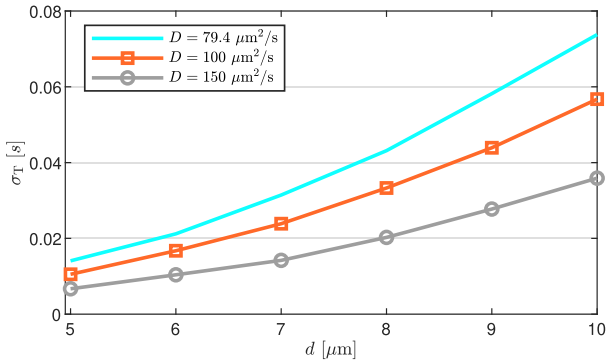

Fig. 4. Standard deviation of T_{peak}.

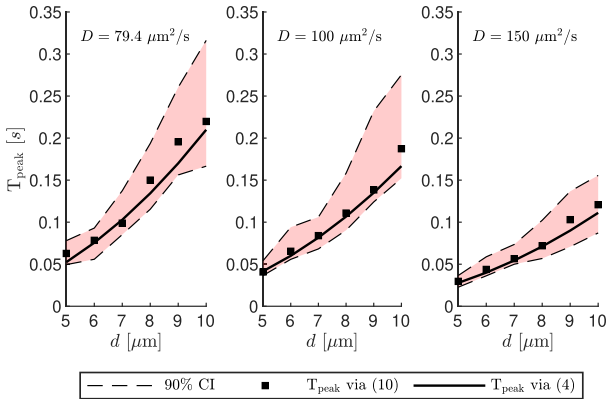

Fig. 5. 90% confidence intervals of T_{peak}. Bootstrap samples were set to L.

In Fig. 5, we can observe that the width of the confidence interval increases with distance and diffusion coefficient stemming from the fact these parameters influence the amount of noise in the measured concentration. That said, we observe that the expected T_{peak} falls within the confidence intervals. Furthermore, we find that the simulated T_{peak} as defined by (11) is in good agreement with the theoretical T_{peak} as defined by (4).

V. Performance Evaluations

In Fig. 6, the cumulative distribution functions (CDFs) of the theoretical models and simulation are presented. We can see that both the distance and the diffusion coefficient affect the estimation accuracy of the models. While the simplicity of the models enables easier mathematical analysis, it is possibly

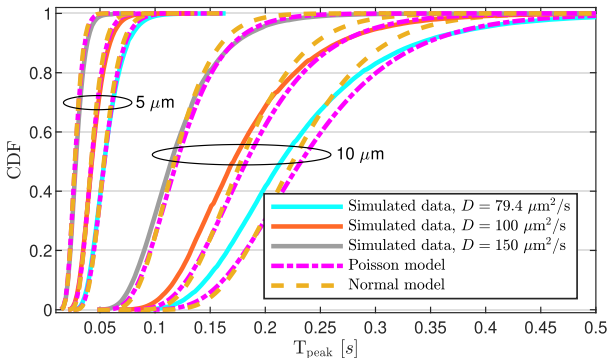

Fig. 6. CDF of T_{peak} from simulation and model.

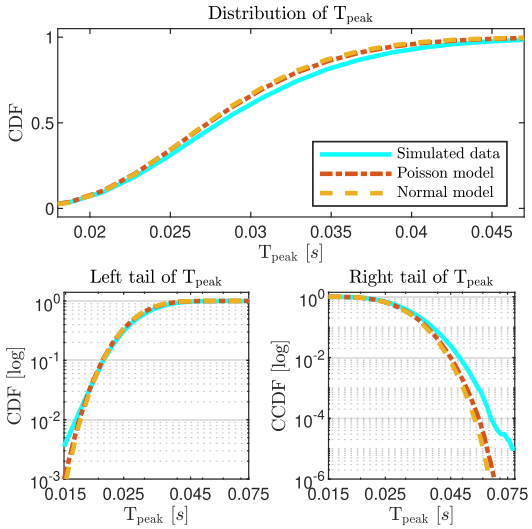

Fig. 7. CDF and survival analysis of best case scenario ($d = 5\ \mu$m and $D = 150\ \mu m^2/s$).

causing the estimation mismatch. For concreteness, we analyze the estimation mismatch patterns by considering two special scenarios — best and worst case. For the best case, we set $d = 5\,\mu$m and $D = 150\mu m^2/s$, while for the worst case we set $d = 10\,\mu$m and $D = 79.4\mu m^2/s$. For a clearer visualization of the fits, we truncate the CDF to extrapolate the middle region of the distribution, and we plot the log-log scale of the CDF and the complementary CDF (CCDF) to extrapolate the left and right tails of the distribution, respectively.

Fig. 7 and Fig. 8 presents the truncated CDFs (top), the log CDF (bottom left), and the log CCDF (bottom right) for best and worst case scenarios, respectively. About the distribution, in the best case (*cf.* Fig. 7), both models overestimate the distribution, while in the worst case (*cf.* Fig. 8) the Poisson model underestimates and the Normal model switches from underestimating to overestimating after $0.25\,$s. About the tails, in the best case, the Poisson model does a slightly better approximation, while in the worst case the Poisson model approximates the data much better. We infer that the Normal model assigns to the extreme tail values probabilities that reduce rapidly. Overall, the extreme values are much more common than the prediction of the models.

Next, we analyze the distance between the CDFs of the data and the models using the normalized sum of the absolute difference in the cumulative distributions (NSADCD) which

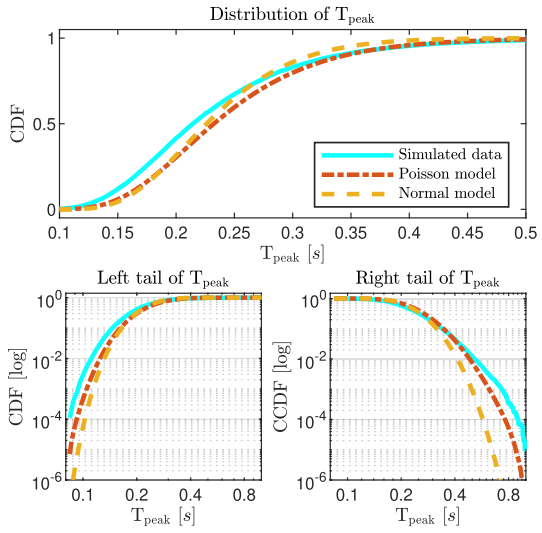

Fig. 8. CDF and survival analysis of worst case scenario ($d = 10\,\mu$m and $D = 79.4\,\mu\text{m}^2/\text{s}$).

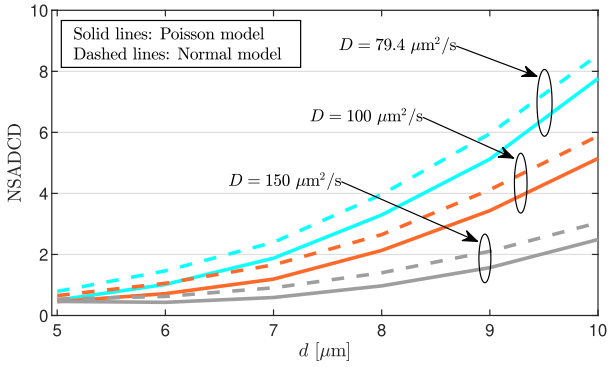

Fig. 9. NSADCD versus distance.

can be written as

$$\text{NSADCD} = \sum_{k=1}^{K} \left| F^{\text{mod}}_{T_{\text{peak}}}[k] - F^{\text{sim}}_{T_{\text{peak}}}[k] \right|, \tag{15}$$

where $F_{T_{\text{peak}}}(x) = \Pr(T_{\text{peak}} \leq x)$ and "mod" denotes the models. From Fig. 9, we observe that the Poisson model's NSADCD is lower than that of the Normal model's. This is expected because the Poisson model performs a better fit, resulting in a smaller difference between its CDF and that of the data. Moreover, we can observe that even with an increase in the measured concentration's noise, the Poisson model captures the distribution much better than the Normal model. Thus, in line with the earlier findings, we can infer that the distribution is asymmetric.

VI. Conclusion

In this letter, we demonstrated that the peak time distribution of the hitting time histogram exhibits a left-skewed heavy right-tail distribution and showed that the expected peak time can be characterized by the mode of the distribution. Poisson and Normal approximations of the absorbed molecules were used to carry out the theoretical analysis, resulting in semi-analytical expressions. The evaluations carried out with the approximated models confirmed that the distribution is asymmetric. Most specifically, the extreme values of the distribution were effectively captured by the Poisson model. The derived formulations can be extended to different types of receiver by plugging in the appropriate $F_{\text{hit}}(d, t)$ formula in (5). With these findings, it is understood that the asymmetric nature of the distribution and its extreme values are essential parameters that must be considered in the development of accurate system models.

References

[1] N. Farsad, H. B. Yilmaz, A. Eckford, C.-B. Chae, and W. Guo, "A comprehensive survey of recent advancements in molecular communication," *IEEE Commun. Surveys Tuts.*, vol. 18, no. 3, pp. 1887–1919, 3rd Quart., 2016.

[2] H. B. Yilmaz, A. C. Heren, T. Tugcu, and C.-B. Chae, "Three-dimensional channel characteristics for molecular communications with an absorbing receiver," *IEEE Commun. Lett.*, vol. 18, no. 6, pp. 929–932, Jun. 2014.

[3] A. Einstein, *Investigations on the Theory of the Brownian Movement*. New York, NY, USA: Dover, 1956.

[4] M. U. Mahfuz, D. Makrakis, and H. T. Mouftah, "On the characterization of binary concentration-encoded molecular communication in nanonetworks," *Nano Commun. Netw.*, vol. 1, no. 4, pp. 289–300, Dec. 2010.

[5] A. Noel and A. W. Eckford, "Asynchronous peak detection for demodulation in molecular communication," in *Proc. IEEE Int. Conf. Commun. (ICC)*, May 2017, pp. 1–6.

[6] M. J. Moore, T. Nakano, A. Enomoto, and T. Suda, "Measuring distance from single spike feedback signals in molecular communication," *IEEE Trans. Signal Process.*, vol. 60, no. 7, pp. 3576–3587, Jul. 2012.

[7] A. Noel, K. C. Cheung, and R. Schober, "Joint channel parameter estimation via diffusive molecular communication," *IEEE Trans. Mol. Biol. Multi-Scale Commun.*, vol. 1, no. 1, pp. 4–17, Mar. 2015.

[8] E. Shitiri, H. B. Yilmaz, and H.-S. Cho, "A time-slotted molecular communication (TS-MOC): Framework and time-slot errors," *IEEE Access*, vol. 7, pp. 78146–78158, 2019.

[9] V. Jamali, A. Ahmadzadeh, and R. Schober, "Symbol synchronization for diffusion-based molecular communications," *IEEE Trans. Nanobiosci.*, vol. 16, no. 8, pp. 873–887, Dec. 2017.

[10] X. Huang, Y. Fang, and N. Yang, "A survey on estimation schemes in molecular communications," *Digit. Signal Process.*, Jul. 2021, Art. no. 103163. [Online]. Available: https://www.sciencedirect.com/science/article/pii/S1051200421002025

[11] S. Kumar, "Nanomachine localization in a diffusive molecular communication system," *IEEE Syst. J.*, vol. 14, no. 2, pp. 3011–3014, Jun. 2020.

[12] T. Nakano, A. W. Eckford, and T. Haraguchi, *Molecular Communication*. Cambridge, U.K.: Cambridge Univ. Press, 2013.

[13] L. Lin, C. Yang, M. Ma, S. Ma, and H. Yan, "A clock synchronization method for molecular nanomachines in bionanosensor networks," *IEEE Sensors J.*, vol. 16, no. 19, pp. 7194–7203, Oct. 2016.

[14] N. Garralda, I. Llatser, A. Cabellos-Aparicio, E. Alarcón, and M. Pierobon, "Diffusion-based physical channel identification in molecular nanonetworks," *Nano Commun. Netw.*, vol. 2, no. 4, pp. 196–204, Dec. 2011.

[15] J. J. Shynk, *Probability, Random Variables, and Random Processes: Theory and Signal Processing Applications*. Hoboken, NJ, USA: Wiley, 2013.

[16] A. Noel, K. Cheung, and R. Schober, "Optimal receiver design for diffusive molecular communication with flow and additive noise," *IEEE Trans. Nanobiosci.*, vol. 13, no. 3, pp. 350–362, Sep. 2014.

[17] S. M. Ross, *Introduction to Probability Models*, 11th ed. San Diego, CA, USA: Academic, 2014.

[18] J. Shi *et al.*, "Optimally estimating the sample standard deviation from the five-number summary," *Res. Synth. Methods*, vol. 11, no. 5, pp. 641–654, Jul. 2020. [Online]. Available: https://onlinelibrary.wiley.com/doi/abs/10.1002/jrsm.1429

[19] F. Dinc, L. Thiele, and B. C. Akdeniz, "The effective geometry Monte Carlo algorithm: Applications to molecular communication," *Phys. Lett. A*, vol. 383, no. 22, pp. 2594–2603, Aug. 2019.

[20] N. Farsad, W. Guo, C. B. Chae, and A. Eckford, "Stable distributions as noise models for molecular communication," in *Proc. IEEE Global Commun. Conf.*, Dec. 2015, pp. 1–6.

[21] B. Efron and R. J. Tibshirani, *An Introduction to the Bootstrap* (Monographs on Statistics and Applied Probability), no. 57. Boca Raton, FL, USA: Chapman & Hall, 1993.